



**Extreme hot days and  
atmospheric  
dynamics**

J. A. García-Valero et al.

This discussion paper is/has been under review for the journal Natural Hazards and Earth System Sciences (NHESS). Please refer to the corresponding final paper in NHESS if available.

# Attributing trends in extremely hot days to changes in atmospheric dynamics

**J. A. García-Valero<sup>1,2</sup>, J. P. Montávez<sup>1</sup>, J. J. Gómez-Navarro<sup>3</sup>, and P. Jiménez-Guerrero<sup>1</sup>**

<sup>1</sup>AEMET, Delegación territorial de Murcia, Murcia, Spain

<sup>2</sup>Department of Physics, University of Murcia, Murcia, Spain

<sup>3</sup>Climate and Environmental Physics, Physics Institute and Oeschger Centre for Climate Change Research, University of Bern, Bern, Switzerland

Received: 7 February 2015 – Accepted: 23 April 2015 – Published: 20 May 2015

Correspondence to: J. P. Montávez (montavez@um.es)

Published by Copernicus Publications on behalf of the European Geosciences Union.

Title Page	
Abstract	Introduction
Conclusions	References
Tables	Figures
◀	▶
◀	▶
Back	Close
Full Screen / Esc	
Printer-friendly Version	
Interactive Discussion	



## Abstract

This paper proposes a method that allows the detection of trends in the frequency of extreme events and its attribution to changes in atmospheric dynamics characterized through Circulation Types (CTs). The method is applied to summer Extremely Hot Days (EHD) in Spain during the period 1958–2008. For carrying out this exercise, regional series of daily maximum temperature are derived from the regional dataset Spain02. Eight regions with different daily maximum temperature variability are identified. All of them exhibit important trends in the occurrence of EHDs, especially in inner regions. Links between the probability of EHD occurrence in the regions and CTs have been calculated. Furthermore, the consistency of the results to the atmospheric variables used in defining the CTs is analyzed. Sea Level Pressure (SLP), Temperature at 850 hPa Level (T850) and Geopotential Height at 500 hPa Level (Z500) from the ERA40 dataset have been used for the six CT classifications obtained using the variables separately and in different combinations of pairs. The optimum choice of large scale variables depends on the region under consideration, being the combination SLP-T850 the one giving the most suitable characterization for most of them. Finally, an attribution exercise of the regional EHD trends to the dynamics is proposed. Results show that the maximum of attributable EHD trends to changes in dynamics in every region is always below 50 %, being even lower than 20 % in those regions with the largest EHD trends, mainly located in the center of the Iberian Peninsula (IP).

## 1 Introduction

Climate suffers changes at different time scales driven by several external and internal factors. Human-induced changes in green-house gases, land use, etc., have been especially prominent in the last centuries, modifying the energy balance and therefore inducing climate changes (Stocker et al., 2013). The attribution of recent climate change to each factor tries to ascertain the causes for recent changes observed in the Earth's

**NHESSD**

3, 3323–3367, 2015

## Extreme hot days and atmospheric dynamics

J. A. García-Valero et al.

Title Page

Abstract

Introduction

Conclusions

References

Tables

Figures



Back

Close

Full Screen / Esc

Printer-friendly Version

Interactive Discussion



climate and quantify their relative relevance. However, although the main factors perturbing the climate at global scale have been extensively characterized (Huybers and Curry, 2006; Swingedouw et al., 2011), less exercises with the focus put on regional scales are available (Stott, 2003).

Beyond the average state, the footprint of climate change is manifested through shifts in extreme weather. Along the last years there has been an increasing interest in quantifying the role of human and other external influences on climate in specific weather events (Stott, 2003; Zwiers et al., 2011). Therefore, trying to attribute extreme events to climate change at regional scales presents particular challenges for science.

In the last decades Europe has experienced a prominent increase in the occurrence of extremely warm episodes, especially during summer time (Frich et al., 2002; Klein Tank and Können, 2003; Alexander et al., 2006). The impacts of such events on human health are important, observing high rates of mortality when such extremes occur. Examples of this are the summers of 2003 (Trigo et al., 2005) and 2010 (Dole et al., 2011), when persistent episodes of high maximum temperatures in western and eastern Europe took place. Several studies show that days exceeding the 95th percentile of the maximum temperature series (extremely hot days) provoke also an increasing in mortality especially among the elderly and people with cardiovascular diseases (Díaz-Jiménez et al., 2005). Many works have tried to investigate the causes of these trends, concluding that these are largely influenced by the anthropogenic activity (Stott, 2003; Zwiers et al., 2011), being summers like that of 2003 expected to become more frequent under several climate change scenarios (Beniston, 2004). However, extreme events are also driven by unpredictable internal variability. Indeed some authors Dole et al. (2011) argued that the summer of 2010 was the result of the internal variability of the climate system, rather than a clear response to global warming.

Many works have analyzed the influence of the large-scale dynamics on the variability of extreme temperature indices using several methodologies. For example, Della-Marta et al. (2007) and Carril et al. (2008) related the influence of the atmosphere dynamics and sea surface temperature (SST) on the heat waves using methods based

## Extreme hot days and atmospheric dynamics

J. A. García-Valero et al.

Title Page

Abstract

Introduction

Conclusions

References

Tables

Figures



Back

Close

Full Screen / Esc

Printer-friendly Version

Interactive Discussion



## Extreme hot days and atmospheric dynamics

J. A. García-Valero et al.

Title Page

Abstract

Introduction

Conclusions

References

Tables

Figures



Back

Close

Full Screen / Esc

Printer-friendly Version

Interactive Discussion



on EOFs or CCA. Other studies use CTs (Yiou and Nogaj, 2004; Yiou et al., 2008; Van den Besselaar et al., 2010; Fernández-Montes et al., 2013). These are guided by the results obtained by Corti et al. (1999) who pointed out that recent climate changes can be interpreted in terms of changes in the frequency of occurrence of natural atmospheric circulation regimes. Some patterns related to anticyclonic and blocking situations favor the development of warm extreme events over Europe (Yiou et al., 2008; Carril et al., 2008; Pfahl, 2014). Therefore, trends in the appearance of these situations can be behind the trends of this kind of events. Many studies using CTs have informed of the increasing observed in the frequency of such patterns since the second half of the past century (Huth, 2001; Kyselý and Huth, 2006; Philipp et al., 2006; Cony et al., 2010; Bermejo and Ancell, 2009; Fernández-Montes et al., 2013; García-Valero et al., 2012). On the other hand, based on the robustness of the evidence from multiple models, the last IPCC report (Stocker et al., 2013) concludes that it is likely that human influence has altered sea level pressure (SLP) patterns globally since 1951. In that way, climate change induces changes in circulation that can further modify extreme events occurrence.

However, not all studies in literature find strong links between trends in the occurrence of extreme episodes and trends in the frequency of CTs. Jones and Lister (2009); Bermejo and Ancell (2009); Fernández-Montes et al. (2013) among others, found that trends in extreme temperatures are mainly due to the increase of temperature within the CTs, rather than the increase of the frequency of occurrence of the CTs. This could suggest that trends in extremes can be in addition linked to other forcings such as: global warming, teleconnection phenomena (El Kenawy et al., 2012; Della-Marta et al., 2007), dryness of soil, increase of the SST, etc. Discrepancies in relating both kind of trends might be provoked by the way CT classifications are built. In general, classifications are obtained using a huge number of days that are clustered in a small number of groups that define the CTs (García-Valero et al., 2012). The great variability existing of the atmospheric patterns causes a reduced signal-to-noise ratio inside the clusters, leading to explain generally less than half of the total variance (Philipp et al., 2006;



links, and the attribution of the EHD trends to the changes of the CTs are explained in Sect. 5. Finally, main conclusions and discussions are in Sect. 6.

## 2 Data

### 2.1 Surface temperature data

5 Several high resolution climate databases for the IP (Herrera et al., 2010) or including it (Caesar et al., 2006; Haylock et al., 2008) have been developed during the last years. These databases have been built by interpolation techniques applied to, in principle, a dense observation network. Although generally reliable, these databases present some known inconsistencies (Gómez-Navarro et al., 2012a) due to differences in the  
10 raw observational series, the interpolation method, or the different quality controls applied to the data.

In this work, we use the maximum daily temperature obtained from Spain02 (Herrera et al., 2010) grid dataset, due to the larger number of stations used compared to other similar products available. The large spatial resolution over mainland Spain and  
15 Balearic islands ( $0.2^\circ \times 0.2^\circ$ ), together with the length of the period (1951–2008), ensures a sufficient spatial and temporal coverage over the study area. Since the work focus on extremely hot days, only dates between 16 June and 15 September are considered.

### 2.2 Large scale atmospheric data

20 The data for characterizing the structure of the atmosphere consist of daily fields at 12:00 UTC of Sea Level Pressure (SLP), Temperature at 850 hPa (T850) and Geopotential Height at 500 hPa level (Z500) extracted from the ERA40 reanalysis (1958–2002) (Uppala et al., 2005) and ECMWF analysis (2003–2008). The maximum common resolution ( $1.125^\circ$ ) is used for the period 1958–2008. The variables considered  
25 are commonly used for the diagnostic of meteorological situations potentially leading

## Extreme hot days and atmospheric dynamics

J. A. García-Valero et al.

Title Page

Abstract

Introduction

Conclusions

References

Tables

Figures



Back

Close

Full Screen / Esc

Printer-friendly Version

Interactive Discussion



to extreme heat events. In this context, SLP offers information about fluxes at low levels, hence informing about the area of provenance of the air mass reaching a given region. T850 informs about the temperature at low atmospheric levels, tightly related to surface temperature (Brands et al., 2011). Finally, Z500 provides a global vision of the mean atmospheric state. Furthermore, it provides some insight about the overall trough and ridge patterns over the study area, indicating large advection and subsidence in the atmosphere (Sheridan et al., 2012).

### 3 Regional series and EHD

This section describes the methodology to identify a set of regions that cluster local series with similar temporal variability of the summer maximum temperature. Spatially averaged regional series filter out local factors and provide a robust characterization of extreme situations affecting the different regions, as well as simplify the exposure of the different behaviors.

#### 3.1 Clustering procedure

The procedure applied is similar to that employed by Jiménez et al. (2008). First, a Principal Component Analysis (Storch and Zwiers, 1999) in S-mode is applied to the correlation matrix obtained from daily anomalies. Only the three first EOFs following the scree plot test (Cattell, 1966) were retained, explaining more than 80% of total variance. Second a two step clustering method is applied to the loadings of each grid point in the retained EOFs. The Ward algorithm (Ward, 1963) is employed for obtaining the number of groups and centroids that are used as seeds for a definitive K-means clustering (Hartigan and Wong, 1979).

## Extreme hot days and atmospheric dynamics

J. A. García-Valero et al.

Title Page

Abstract

Introduction

Conclusions

References

Tables

Figures



Back

Close

Full Screen / Esc

Printer-friendly Version

Interactive Discussion



## 3.2 Regions

The aim of this study is not to perform an exhaustive analysis of the regions, but rather to use the regional series as a tool for achieving the final target, so only some aspects related to the time variability are presented below. Figure 1 shows the eight regions obtained by the clustering procedure. The name of regions has been established according to their geographical locations: SW, NE, E, Cs, NWs, NWe, NWw and N. Regional series have been constructed by averaging the time series of all the grid points belonging to the same region. Table 1 (first four columns) shows some statistics of the regional series: mean, trend, standard deviation and 95th percentile. A meridional gradient of mean and percentile values is observed, being the warmest regions located in the southern half of the country (SW and Cs). In addition, distance to the sea is another factor influencing the maximum temperature spatial distribution. Inner regions are warmer and have higher standard deviation. Some examples are NWs and NE regions in the northern half, and Cs in the South.

The temporal variability of the regional series is analysed in Fig. 2, that shows the seasonal mean series (solid black curve). As previously pointed out by Brunet et al. (2007) for the IP, as well as for other further Mediterranean regions Burić et al. (2014), two periods with different behaviour stands out in all regions. The first lies between 1951 and 1977, when temperatures dropped significantly, being 1977 the coldest year for most regions. The second period (1978–2007) is characterized by a significant rise of the maximum temperatures. The 90's decade was especially warm, occurring the hottest year for most regions. In particular, 1994 was the hottest for eastern (NE, E and Cs), 1991 for western (SW and NWs) and 1990 for northern regions. During the last decade, it is observed changes of the standard deviation of the regional series, decreasing over the central, southern and eastern regions, whereas increasing in northern areas (N, NWe and NWw).

## Extreme hot days and atmospheric dynamics

J. A. García-Valero et al.

Title Page

Abstract

Introduction

Conclusions

References

Tables

Figures



Back

Close

Full Screen / Esc

Printer-friendly Version

Interactive Discussion



### 3.3 Extremely hot days

In this work, a day is defined as Extremely Hot Day (EHD) when the maximum regional temperature series exceeds its 95th percentile in any of the regional series (values in the 5th column of Table 1). A total of 863 EHDs were identified for this study.

Some aspects related to annual variability of the regional EHDs series, as well as a comparison of simultaneous occurrence of EHD among the different regions, have been analyzed. Annual number of EHD for the various regions are shown by vertical bars in Fig. 2. All regions show a noticeable increase in EHDs since the 90s. This finding agrees with those obtained for the IP by Brunet et al. (2007) and Fernández-Montes et al. (2013) as well as for Europe by Klein Tank and Können (2003). Thus, positive and significant trends are obtained in all regions (Table 1), being the trends larger in the inner regions (NE, Cs, NWs). It is noteworthy that the year with the highest number of EHDs depends on the region. The year with the maximum number of EHDs is 2003 for the northern regions (N, NWe, NWs and NE). This is not surprising since it coincides with the extraordinary heat wave occurred in many places of western Europe (Beniston, 2004; Trigo et al., 2005). Furthermore, this event is also characterized by a great persistence. NE, N, NWe, NWs and SW regions suffered EHD persistences up to 10 days (NE, N, NWe, NWs) and 16 days (SW). The maximum number of EHDs took place in the early 90s in the rest of the regions. Curiously, in the E region, the maximum of EHD occurred in two consecutive years (1958 and 1959).

A trend analysis of the seasonal EHD series (6th column of Table 1) was performed using the Sen's algorithm (Sen, 1968) using the period 1958–2008. All regions have positive and significant trends at 95 % (significances obtained by the Mann–Kendall test), but E and NWe that are significant at 90 %. The inner regions show the larger trends (Cs, NWs and NE), a similar warming pattern to that obtained by Bermejo and Ancell (2009) and Gómez-Navarro et al. (2010) for the second half of the past century for summer maximum temperatures.

## Extreme hot days and atmospheric dynamics

J. A. García-Valero et al.

Title Page

Abstract

Introduction

Conclusions

References

Tables

Figures



Back

Close

Full Screen / Esc

Printer-friendly Version

Interactive Discussion



---

## Extreme hot days and atmospheric dynamics

J. A. García-Valero et al.

---

Title Page

Abstract

Introduction

Conclusions

References

Tables

Figures

⏪

⏩

◀

▶

Back

Close

Full Screen / Esc

Printer-friendly Version

Interactive Discussion



One important aspect to study is how different is the behavior of EHD among the different regions. Table 2 shows the probability of having simultaneous occurrences of EHDs between pairs of regions. The diagonal values are the probability of occurrence of an EHD in only one region. The region which has the most independent behavior is E region (40 %), while NWs shares many episodes with many other regions (5 %). The lowest probability of simultaneous EHD occurrences is for E and NWs (15 %), while the largest is for NWs and SW (62 %). In general, there are important regional differences, which points to the conclusion that a given large atmospheric pattern should provoke different behaviors along the various regions.

## 4 Characterization of EHDs circulation types

As discussed above, the links between EHD occurrences and CTs can be hampered by the low signal-to-noise ratio that most CT classifications present, since they are usually obtained considering all days within a long extended period of time. For our purpose, it is more reasonable to obtain the CT classification using only extreme days, i.e, to characterize the atmospheric circulation that drives these extreme situations. On the other hand, such links could be sensitive to the large scale atmospheric variables used for the CT classification. Hence, in this section we construct the CTs using only the days classified as EHD and different combinations of large scale atmospheric variables and analyze the links between EHD occurrence and the CTs, trying to identify the most suitable set of atmospheric variables for characterizing the EHDs.

### 4.1 CT Classification procedure

The clustering method followed for the CT classifications is the same employed in Kyselý and Huth (2006) and García-Valero et al. (2012). It bases on a two step procedure. First a PC-ModeT clustering is applied to the Rotated Empirical Orthogonal Functions (REOF) obtained from the retained EOFs of the T-Mode. A scree plot test (Cattell,

1966) is used to select the number of retained modes. This step provides the centroids (composites of the anomalies of each cluster) that are projected over the PCs retained in the S-mode. Then, this projections are used as initial seeds to initialize the second step: a K-means clustering.

5 The input for the clustering procedure consist of the atmospheric situations for the 784 days classified as EHD within the period (1958–2008). The spatial window considered for the classifications covers enterely the IP (35–45° N and 10° W–6° E) and it is formed by 150 grid points. This configuration is identical to that used in García-Valero et al. (2012). A larger spatial window is used to represent the centroids.

10 For the identification of the optimal atmospheric variables in representing the EHDs, six different CTs classifications are obtained. Three of them consider the atmospheric variables individually (SLP, T850 and Z500). In this case, each classification is formed by six clusters (being this number the double of the retained PCs, García-Valero et al., 2012). The other three classifications consider all possible pairs of variables: SLP-T850  
15 (Fig. 3), SLP-Z500 (Fig. 5) and Z500-T850 (Fig. 4), and they are formed by eight (four retained PCs) clusters each one. In all cases the retained PCs explains nearly the 90 % of the total variance.

## 4.2 Evaluation of the CT classifications for EHD description

In the ensemble of the EHDs clustered in the six obtained CTs classifications, there are days that are extremes for one or various regions but not for the other regions, and vice versa. Therefore, within a given CT classification, there are some CTs more related to the occurrence of EHDs in some regions. An important question is whether for a given region there is, among the six classifications, anyone that discriminates better the EHD occurrence. In order to address this question an effectiveness index (EI) is defined.  
20 This index is calculated as the ratio between the number of EHD occurrences and non occurrences in the region under a given CT. Therefore, for a given CT classification and region, there is a set of EIs. We define as best CT classification whose the standard

## Extreme hot days and atmospheric dynamics

J. A. García-Valero et al.

Title Page

Abstract

Introduction

Conclusions

References

Tables

Figures



Back

Close

Full Screen / Esc

Printer-friendly Version

Interactive Discussion



deviation and range of the EIs are the largest, since it separates better the most from the less influential CTs.

Table 3 shows the range and standard deviation (range-sd) obtained for all the regions and CT classifications. Last column shows the best (highlighted in black) CT classification, as well as their extreme CTs for each region. Results indicate that two synoptic variables characterize better the EHDs for most regions. Z500-T850 is the best one for NE, NWw and Cs (inner-eastern regions and northwestern). SLP-Z500 characterizes better E region. SLP-T850 is the best for SW, NWe and N (western and northern regions). T850 classification is the best for the NWs region. However, in this area SLP-T850 perform quite similar. Hence, and for the shake of clarity in the analysis, SLP-T850 has been considered as the best classification in this case. Figures 3–5 show all the CTs (contours) of the best CT classifications and the efficiencies for each region (shaded). Efficiency is defined as the conditional probability of having an EHD in a region under a given CT. Another interesting parameter is the contribution of a given CT to the occurrence of the EHDs in a given region. The contribution is assessed by calculating the ratio between the number of observed EHDs under a CT and the total EHDs observed in a region. Tables 4 and 5 depict the efficiencies and contributions values.

The efficiency patterns are quite similar for the three CT classifications. However, for each region the efficiency is larger for the classification that gives larger spreads in the EI index (Table 3). Some examples follow. The efficiency pattern related to CT8 is equivalent in all classifications and shows high efficiency over the E region. The efficiency is larger for the SLP-Z500 classification which has the largest EI index for E region. Similar results are found for CT5-SLP-T850, CT6-Z500-T850 (best) and CT5-SLP-Z500 in the NWw region, and for CT3-SLP-T850 (best), CT3-Z500-T850 and CT1-SLP-Z500 over the SW region. These results suggest that some CTs belonging to different classifications are equivalent, ie. they give similar efficiency patterns. In fact, this can be corroborated by calculating the common days of the mentioned CTs (not

## Extreme hot days and atmospheric dynamics

J. A. García-Valero et al.

Title Page

Abstract

Introduction

Conclusions

References

Tables

Figures



Back

Close

Full Screen / Esc

Printer-friendly Version

Interactive Discussion



shown). This highlights the need of studies on the sensitivity of the CT classification to the atmospheric variables employed.

The comparison of the atmospheric situations among the different classification associated with similar spatial efficiency patterns, enables to draw conclusions about the main drivers related to the EHD occurrences. Regarding the T850 variable, the regional efficiency shows the highest values at regions where temperatures are near and above 20°C. This feature is very common in many CTs of the different classifications such as the CTs-2/3/4/6/8 of SLP-T850 and the CTs-1/2/3/4/5/7/8 of the Z500-T850 classification. The wind provenance, inferred considering the SLP field, is also an important factor contributing the occurrence of EHDs in some regions, because of the warm advection over specific regions. Many CTs are related to situations when wind blows from inner towards coastal areas, provoking the highest efficiencies in the latter. The inner IP regions are high land plateau areas where the highest temperatures are observed (see Table 1). When wind blows from this area towards the sea along valleys, air is adiabatically compressed causing an important warming at low land regions. Some examples of these situations can be identified in the classifications by analyzing the efficiencies and contributions of some CTs. Five regions are mainly affected by this. NWw, especially when wind blows from the East because of the presence of High Pressures over western Europe (CT5 of SLP-T850 and SLP-Z500). SW in northeastern winds conditions (CTs-1/3 of SLP-T850 and CT1 of SLP-Z500) as result of the presence of high pressure over the Mediterranean and relative low pressures over the southwest of the IP. The E region under strong western zonal wind (CT8 of SLP-T850 and SLP-Z500), induced by the location of High/Low pressures over the Atlantic/Mediterranean. The NE and N regions in southwestern winds situations (CT6 of SLP-T850 and SLP-Z500). Conversely, CTs with weak SLP gradients (stagnant situations linked to thermal lows) are especially important in the EHD occurrences at Cs and NE (CT4 of SLP-T850 and SLP-Z500), and N, NWe and NWs (CT2 SLP-T850) regions. Such situations were also pointed out by Pfahl (2014) like those more relevant guiding hot extremes at summer in the IP. Regarding the Z500 field, EHDs are associated with large amplitude ridges

**Extreme hot days and atmospheric dynamics**

J. A. García-Valero et al.

Title Page

Abstract

Introduction

Conclusions

References

Tables

Figures



Back

Close

Full Screen / Esc

Printer-friendly Version

Interactive Discussion





et al., 2012; Vautard and Yiou, 2009) whereas the latter evaluates the differences in the intensity of patterns (Fettweis et al., 2011). Both metrics are relevant and complementary (Nogaj et al., 2007; Fettweis et al., 2011). The population of a given CT will be characterized by the distribution of the distances to and correlations with the centroid.

A criterium to allocate a situation in a given CT is that the distance to/correlation with the centroid be lower/higher than some given thresholds. The most objective election of thresholds is the maximum distance and the minimum correlation of the population for each CT. Table 6 shows the thresholds chosen for all CTs.

Prior to the allocation process, all days and centroids are standardized at each grid point. A day is allocated in a given CT when both, distance and correlation, are lower and higher, respectively, than a defined threshold value for each one. Days that are not allocated in any CT are assigned to a new group (unclassified group, CT9) (Seubert et al., 2014). It is possible to find atmospheric situations that can be assigned to several clusters. In these cases, they are allocated to the nearest cluster considering the euclidean distance. The use of the euclidean distance as definitive criteria obeys mainly to the lower variance of the distance population.

## 5.2 Results of the allocation

Table 8 shows the number of days belonging to the different CTs before/after the allocation process. Approximately 70 % of the days for all classifications are assigned, whereas the rest are allocated into the unclassified cluster (CT9), being Z500-T850 (SLP-Z500) the one with more (least) unclassified days (33 vs. 28 %). There is a large variability in the increase of the days belonging to the different CTs. CT1, CT6 and CT8 have the largest increase (10 times) in all classifications, whereas others like CT2/4-SLP-T850 and CT2/4-Z500-T850 present small changes (less than 20 % of the initial clustered days).

In order to ensure the reliance of the method, the measure of the quality of the clusters before and after the allocation is of major relevance. The explained cluster variance (ECV) of each classification (Table 7) is analyzed, obtaining small differences

## Extreme hot days and atmospheric dynamics

J. A. García-Valero et al.

Title Page

Abstract

Introduction

Conclusions

References

Tables

Figures



Back

Close

Full Screen / Esc

Printer-friendly Version

Interactive Discussion



in all cases. Z500-T850 classification has the best quality, producing even an increase in the quality of clusters after the allocation. The quality of the other classifications worsen slightly after the allocation, being the SLP-T850 classification slightly better than the SLP-Z500. On the other hand, the quality of all classifications after the allocation are of the same order than other classifications (summer) such as those obtained in Philipp et al. (2006) (ECV < 40 %) and García-Valero et al. (2012) (47.2 %). These results support the suitability of the criterion used for defining the thresholds in the allocation method, making not necessary the choice of others more restrictive and not exempts from subjectivity.

It is instructive to explore the consequences on the properties of the groups after applying the allocation procedure. One consequence of the larger number of classified days, is the decrease in the efficiency of the CTs (see Table 4). Obviously, the lower increase of number of days, the lesser decrease of the efficiency. This effect stands out in CT-2/4 for the SLP-T850 and Z500-T850 classifications, which have the highest efficiencies in most regions. The shape of the population distribution of the distances and correlation in each CT can be also affected. The effect of the allocation process is to include new days located further from the centroid. Nevertheless, a small number of clusters hardly change the populations after the assignation (CT2-4-SLP-T850, CT-2/4-Z500-T850 and CT-4/7-SLP-Z500) which are coincident with the ones with higher efficiency. Figure 6 shows two examples of the correlation histograms before and after the allocation process and their overlap (top) and the empirical cumulative distribution function (bottom). Left/right panels show an example of great/small changes in population.

The most efficient CTs for several regions are the patterns better identified in the characterization step (with more restrictive thresholds, Table 6) and therefore are less sensitive to the allocation process. Changes in the efficiency after the allocation also affect the EI index used for deciding the best CT classification for each region (Sect. 4.2). Following the same criterion as above, results keep unaltered for most regions, but for

## Extreme hot days and atmospheric dynamics

J. A. García-Valero et al.

Title Page

Abstract

Introduction

Conclusions

References

Tables

Figures



Back

Close

Full Screen / Esc

Printer-friendly Version

Interactive Discussion



the E and NWw regions, which are now better characterized by the SLP-T850 classification.

Seasonal trends in the frequency of the CTs are also affected by the allocation. Table 9 shows the trends before/after the allocation obtained by using the Sen trend estimator as well as their statistical significances considering the Mann–Kendall test. Nevertheless, those CTs with higher efficiency in the EHD occurrence remains almost unchanged, CT2 for all classifications.

Attending to these results, and considering all classifications, significant trends in CTs frequency contribute more to a higher frequency of EHDs in northern regions, mainly at N and NE.

### 5.3 Attribution of trends

Temperature changes can be linked to several factors, being one of them the changes in the frequency of the CTs. Trends in the EHDs could be considered also as an indicator of temperature changes. In this subsection, a simple attribution model of the EHDs trends to the trends in the CTs frequency appearance is presented.

The trend in EHD in a given region  $T^r$  can be written as the sum of two terms:

$$T^r = T_c^r + T_o^r \quad (1)$$

where  $T_c^r$  is the trend attributable to changes in atmospheric circulation and  $T_o^r$  the trend related to other factors. Now,  $T_c^r$  can be described as a linear function of the changes in the frequency of the CTs. We propose the simple model:

$$T_c^r = \sum_{i=1}^n T_i e_i^r \quad (2)$$

where the subscript  $i$  denotes the CT number, from 1 to  $n$  (the number of CTs),  $T_i$  is the frequency trend of the CT $_i$  and  $e_i^r$  denotes the efficiency of the CT $_i$  over the region  $r$ , calculated after the allocation process.

## Extreme hot days and atmospheric dynamics

J. A. García-Valero et al.

Title Page

Abstract

Introduction

Conclusions

References

Tables

Figures

◀

▶

◀

▶

Back

Close

Full Screen / Esc

Printer-friendly Version

Interactive Discussion



Using this simple model  $T_c^r$  can be calculated for all regions using the CT classifications obtained above. The results are summarized in Table 10. The fourth column depicts the observed regional trend. The trends reproduced by this simple model are smaller than the observed, also appearing an important variability among the regions.

For most regions the reproduced trends strongly depends on the CT classification, but few differences appears in the SW and NWw regions. In general terms, the Z500-T850 classification obtains the biggest reproduced trends but for NWw. Using this classification a fraction between 40–50 % of the observed trends is attributed in the E, NE, NWE and N regions, about 20 % in the western and southern regions (SW, Cs and NWs) and hardly 14 % in the NWw to changes in the atmospheric dynamics.

#### 5.4 Efficiency of within type variations

Previous works analyze the Within Type (WT) variations of the maximum and minimum temperatures inside the CTs (Fernández-Montes et al., 2013; Bermejo and Ancell, 2009; Jacobeit et al., 2009). They show that many CTs warms during the second half of the past century, observing a higher warming for minimum than for maximum temperatures for the Iberian Peninsula. WT variations are a signal of the changes in the physical links between dynamics and regional variability that at the same time could be modulated by other mechanisms (soil moisture, sea surface temperature, etc.). Thus, in order to evaluate the stability of the relationships between the CTs and EHDs, the possible existence of WT variations in the efficiency of the CTs in each region has been analyzed. For the analysis the moving average efficiency series (31 year) of the best classification for each region has been calculated (Fig. 7).

In general, the CTs related to the highest efficiencies in each region increase its efficiency by 10 % along the study period (1958–2008). This is the case of CT2 in the regions Cs, NWs, NWE, NWw and N, and CT4 in the E region. There are some other important WT variations affecting the inner regions, pointing out to a rise of the efficiency. Some examples follows: CT-3/4 for Cs, CT-1/2 for SW and CT-1/3/7 for NWs.

### Extreme hot days and atmospheric dynamics

J. A. García-Valero et al.

Title Page

Abstract

Introduction

Conclusions

References

Tables

Figures



Back

Close

Full Screen / Esc

Printer-friendly Version

Interactive Discussion



However, CT4 shows an efficiency decrease in the northern regions (NWw, NWe and N), although the efficiency increases in the E region.

NE region is the least affected by WT variations. Only CT1 increases its efficiency, but it is low over the region. Other authors (Bermejo and Ancell, 2009) found that this area has experienced the highest trends in mean maximum temperatures of the IP, attributing such trends to WT variations.

One of the reasons of the efficiency growth of some CTs can be the increase in the persistence. Thus, the higher the persistence of a CT leading EHD, the higher the temperature rises. Hence, the persistence of hot situations favors the development of land-atmosphere positive feedbacks that enhance the air temperature (Jerez et al., 2012; Seneviratne et al., 2010). To evaluate this possible influence, the correlation between the de-trended seasonal frequency series and the mean seasonal persistence series of the CTs with the most important WT have been calculated. Results show positive and significant correlations, between 0.6 and 0.7, which support the influence of the persistence on the efficiency rise. In addition, the decline of soil moisture observed over the IP since 1970s (Sousa et al., 2011) can be an additional factor contributing to this feedback process.

## 6 Conclusions and discussions

This study characterizes the Circulation Types leading summer EHDs occurrence over Spain, defining the EHDs as those when 95th percentile of the maximum daily temperature series is exceeded. For that, a regionalization of maximum daily temperatures in summer have been carried out. The analysis of regional series shows the existence of positive trends in the EHD seasonal frequency in all regions. For the characterization of the CTs three atmospheric variables, SLP, T850 and Z500, have been considered for building six CT classifications, three for the variables used individually and other three using all combination of pairs. The different classifications have been compared for each region in order to identify which explains better its EHD occurrences. In addition,

## Extreme hot days and atmospheric dynamics

J. A. García-Valero et al.

Title Page

Abstract

Introduction

Conclusions

References

Tables

Figures



Back

Close

Full Screen / Esc

Printer-friendly Version

Interactive Discussion







soil moisture that enhances the positive land-atmospheric feedback. This also support the WT variations mentioned above.

The relationship between EHDs and CTs, as well as the allocation methodology presented, can be used as a base for a statistical downscaling method that enables EHD forecast, as well as in regional climate change experiments. In the latter case, WT variations could be a drawback, however in this particular case the changes in the efficiencies are small and therefore, the uncertainty related to WT could be less than the one related to other factors such as the global circulation models or the scenario.

The general methodology applied here could be extended to other variables or types of events such as floods, droughts, heat waves, cold events, etc. The robustness of the regional series as well as the identification of the best large-scale atmospheric variables characterizing such events could be of crucial importance when trying to relate regional extreme behavior to atmospheric dynamics. In addition, an extension of this methodology can be applied to obtain regional climate change escenarios of extreme events.

*Acknowledgements.* This study was supported by the Spanish government and the Fondo Europeo de Desarrollo Regional (FEDER) through the projects SPEQTRES (CGL2011-29672-C02-02) and REPAIR (CGL2014-59677-R). P. Jimenez-Guerrero thanks the Ramon y Cajal Program of the Spanish Ministry of Science and Innovation. The authors also thank to Sonia Fernandez-Montes and the anonymous reviewers for their constructive suggestions.

## References

Alexander, L., Zhang, X., Peterson, T., Caesar, J., Gleason, B., Klein Tank, A., Haylock, M., Collins, D., Trewin, B., Rahimzadeh, F., Tagipour, A., Rupa, K., Revadekar, J., Griffiths, G., Vincent, L., Stephenson, D. B., Burn, J., Aguilar, E., Brunet, M., Taylor, M., New, M., Zhai, P., Rusticucci, M., and Vazquez-Aguirre, J. L.: Global observed changes in daily climate extremes of temperature and precipitation, *J. Geophys. Res.-Atmos.*, 111, D05109, doi:10.1029/2005JD006290, 2006. 3325

## Extreme hot days and atmospheric dynamics

J. A. García-Valero et al.

Title Page

Abstract

Introduction

Conclusions

References

Tables

Figures



Back

Close

Full Screen / Esc

Printer-friendly Version

Interactive Discussion



---

**Extreme hot days and  
atmospheric  
dynamics**


---

 J. A. García-Valero et al.
 

---

[Title Page](#)
[Abstract](#)
[Introduction](#)
[Conclusions](#)
[References](#)
[Tables](#)
[Figures](#)
[⏪](#)
[⏩](#)
[◀](#)
[▶](#)
[Back](#)
[Close](#)
[Full Screen / Esc](#)
[Printer-friendly Version](#)
[Interactive Discussion](#)


Beniston, M.: The 2003 heat wave in Europe: a shape of things to come?, An analysis based on Swiss climatological data and model simulations, *Geophys. Res. Lett.*, 31, L02202, doi:10.1029/2003GL018857, 2004. 3325, 3331

Bermejo, M. and Ancell, R.: Observed changes in extreme temperatures over Spain during 1957–2002, using Weather Types, *Revista de Climatología*, 9, 45–61, 2009. 3326, 3331, 3340, 3341, 3342

Brands, S., Taboada, J., Cofino, A., Schneider, C., Brands, S., Taboada, J. J., Cofiño, A. S., Sauter, T., and Schneider, C.: Statistical downscaling of daily temperatures in the NW Iberian Peninsula from global climate models: validation and future scenarios, *Clim. Res.*, 48, 163–176, 2011. 3329

Brunet, M., Jones, P., Sigró, J., Saladié, O., Aguilar, E., Moberg, A., Della-Marta, P., Lister, D., Walther, A., and López, D.: Temporal and spatial temperature variability and change over Spain during 1850–2005, *J. Geophys. Res.*, 112, D12117, doi:10.1029/2006JD008249, 2007. 3327, 3330, 3331

Burić, D., Luković, J., Ducić, V., Dragojlović, J., and Doderović, M.: Recent trends in daily temperature extremes over southern Montenegro (1951–2010), *Nat. Hazards Earth Syst. Sci.*, 14, 67–72, doi:10.5194/nhess-14-67-2014, 2014. 3330

Caesar, J., Alexander, L., and Vose, R.: Large-scale changes in observed daily maximum and minimum temperatures: creation and analysis of a new gridded data set, *J. Geophys. Res.-Atmos.*, 111, D05101, doi:10.1029/2005JD006280, 2006. 3328

Carril, A. F., Gualdi, S., Cherchi, A., and Navarra, A.: Heatwaves in Europe: areas of homogeneous variability and links with the regional to large-scale atmospheric and SSTs anomalies, *Clim. Dynam.*, 30, 77–98, 2008. 3325, 3326

Cattell, R. B.: The scree test for the number of factors, *Multivar. Behav. Res.*, 1, 245–276, 1966. 3329, 3332

Cony, M., Martín, L., Hernández, E., and Del Teso, T.: Synoptic patterns that contribute to extremely hot days in Europe, *Atmósfera*, 23, 295–306, 2010. 3326

Corti, S., Molteni, F., and Palmer, T.: Signature of recent climate change in frequencies of natural atmospheric circulation regimes, *Nature*, 398, 799–802, 1999. 3326

Della-Marta, P., Luterbacher, J., Von Weissenfluh, H., Xoplaki, E., Brunet, M., and Wanner, H.: Summer heat waves over western Europe 1880–2003, their relationship to large-scale forcings and predictability, *Clim. Dynam.*, 29, 251–275, 2007. 3325, 3326

---

**Extreme hot days and  
atmospheric  
dynamics**


---

 J. A. García-Valero et al.
 

---

[Title Page](#)
[Abstract](#)
[Introduction](#)
[Conclusions](#)
[References](#)
[Tables](#)
[Figures](#)
[◀](#)
[▶](#)
[◀](#)
[▶](#)
[Back](#)
[Close](#)
[Full Screen / Esc](#)
[Printer-friendly Version](#)
[Interactive Discussion](#)


Díaz-Jiménez, J., Linares-Gil, C., and García-Herrera, R.: Impacto de las temperaturas extremas en la salud pública: futuras actuaciones, *Rev. Esp. Salud Public.*, 79, 145–157, 2005. 3325

Dole, R., Hoerling, M., Perlwitz, J., Eischeid, J., Pegion, P., Zhang, T., Quan, X.-W., Xu, T., and Murray, D.: Was there a basis for anticipating the 2010 Russian heat wave?, *Geophys. Res. Lett.*, 38, L06702 doi:10.1029/2010GL046582, 2011. 3325

El Kenawy, A., López-Moreno, J. I., and Vicente-Serrano, S. M.: Recent trends in daily temperature extremes over northeastern Spain (1960–2006), *Nat. Hazards Earth Syst. Sci.*, 11, 2583–2603, doi:10.5194/nhess-11-2583-2011, 2011. 3327

El Kenawy, A., López-Moreno, J. I., and Vicente-Serrano, S. M.: Trend and variability of surface air temperature in northeastern Spain (1920–2006): linkage to atmospheric circulation, *Atmos. Res.*, 106, 159–180, 2012. 3326

Fernández-Montes, S., Rodrigo, F. S., Seubert, S., and Sousa, P. M.: Spring and summer extreme temperatures in Iberia during last century in relation to circulation types, *Atmos. Res.*, 127, 154–177, 2013. 3326, 3331, 3340, 3342

Fettweis, X., Mabilie, G., Ericum, M., Nicolay, S., and den Broeke, M.: The 1958–2009 Greenland ice sheet surface melt and the mid-tropospheric atmospheric circulation, *Clim. Dynam.*, 36, 139–159, 2011. 3337

Font-Tullot, I.: *Climatología de España y Portugal*, University of Salamanca, Spain, 2000. 3327

Frich, P., Alexander, L., Della-Marta, P., Gleason, B., Haylock, M., Klein-Tank, A., and Peterson, T.: Observed coherent changes in climatic extremes during the second half of the twentieth century, *Clim. Res.*, 19, 193–212, 2002. 3325

García-Valero, J., Montavez, J., Jerez, S., Gómez-Navarro, J., Lorente-Plazas, R., and Jiménez-Guerrero, P.: A seasonal study of the atmospheric dynamics over the Iberian Peninsula based on circulation types, *Theor. Appl. Climatol.*, 110, 291–310, doi:10.1007/s00704-012-0623-0, 2012. 3326, 3327, 3332, 3333, 3338

Giorgi, F.: Climate change hot-spots, *Geophys. Res. Lett.*, 33, L08707, doi:10.1029/2006GL025734, 2006. 3327

Gómez-Navarro, J., Montáñez, J., Jimenez-Guerrero, P., Jerez, S., Garcia-Valero, J. A., and González-Rouco, J.: Warming patterns in regional climate change projections over the Iberian Peninsula, *Meteorol. Z.*, 19, 275–285, 2010. 3331

---

**Extreme hot days and  
atmospheric  
dynamics**


---

J. A. García-Valero et al.

[Title Page](#)
[Abstract](#)
[Introduction](#)
[Conclusions](#)
[References](#)
[Tables](#)
[Figures](#)




[Back](#)
[Close](#)
[Full Screen / Esc](#)
[Printer-friendly Version](#)
[Interactive Discussion](#)


- Gómez-Navarro, J., Montávez, J., Jerez, S., Jiménez-Guerrero, P., and Zorita, E.: What is the role of the observational dataset in the evaluation and scoring of climate models?, *Geophys. Res. Lett.*, 39, L24701, doi:10.1029/2012GL054206, 2012a. 3327, 3328
- Gómez-Navarro, J. J., Montávez, J. P., Jiménez-Guerrero, P., Jerez, S., Lorente-Plazas, R., González-Rouco, J. F., and Zorita, E.: Internal and external variability in regional simulations of the Iberian Peninsula climate over the last millennium, *Clim. Past*, 8, 25–36, doi:10.5194/cp-8-25-2012, 2012b. 3327
- Hartigan, J. A. and Wong, M. A.: Algorithm AS 136: a k-means clustering algorithm, *J. Roy. Stat. Soc. C-App.*, 28, 100–108, 1979. 3329
- Haylock, M., Hofstra, N., Klein Tank, A., Klok, E., Jones, P., and New, M.: A European daily high-resolution gridded data set of surface temperature and precipitation for 1950–2006, *J. Geophys. Res.-Atmos.*, 113, D20119, doi:10.1029/2008JD010201, 2008. 3328
- Herrera, S., Gutiérrez, J., Ancell, R., Pons, M., Fías, M., and Fernández, J.: Development and analysis of a 50-year high-resolution daily gridded precipitation dataset over Spain (Spain02), *Int. J. Climatol.*, 32, 74–85, doi:10.1002/joc.2256, 2010. 3327, 3328, 3361
- Hertig, E., Seubert, S., and Jacobeit, J.: Temperature extremes in the Mediterranean area: trends in the past and assessments for the future, *Nat. Hazards Earth Syst. Sci.*, 10, 2039–2050, doi:10.5194/nhess-10-2039-2010, 2010. 3327
- Hofer, D., Raible, C., Merz, N., Dehnert, A., and Kuhlemann, J.: Simulated winter circulation types in the North Atlantic and European region for preindustrial and glacial conditions, *Geophys. Res. Lett.*, 39, L15805, doi:10.1029/2012GL052296, 2012. 3336
- Huth, R.: Disaggregating climatic trends by classification of circulation patterns, *Int. J. Climatol.*, 21, 135–153, 2001. 3326
- Huybers, P. and Curry, W.: Links between annual, Milankovitch and continuum temperature variability, *Nature*, 441, 329–332, 2006. 3325
- Jacobeit, J., Rathmann, J., Philipp, A., and Jones, P. D.: Central European precipitation and temperature extremes in relation to large-scale atmospheric circulation types, *Meteorol. Z.*, 18, 397–410, 2009. 3340
- Jerez, S., Montavez, J., Gómez-Navarro, J., Lorente-Plazas, R., García-Valero, J., and Jiménez-Guerrero, P.: A multiphysic ensemble of regional climate change projections over the Iberian Peninsula, *Clim. Dynam.*, 41, 1749–1768, doi:10.1007/s00382-012-1551-5, 2012. 3341, 3343

- Jiménez, P., García-Bustamante, E., González-Rouco, J., Valero, F., Montávez, J., and Navarro, J.: Surface wind regionalization in complex terrain, *J. Appl. Meteorol. Clim.*, 47, 308–325, 2008. 3329
- Jones, P. D. and Lister, D. H.: The influence of the circulation on surface temperature and precipitation patterns over Europe, *Clim. Past*, 5, 259–267, doi:10.5194/cp-5-259-2009, 2009. 3326
- Klein Tank, A. and Können, G.: Trends in indices of daily temperature and precipitation extremes in Europe, 1946–99, *J. Climate*, 16, 3665–3680, 2003. 3325, 3331
- Kysely, J. and Huth, R.: Changes in atmospheric circulation over Europe detected by objective and subjective methods, *Theor. Appl. Climatol.*, 85, 19–36, 2006. 3326, 3332
- Lorente-Plazas, R., Montávez, J., Jimenez, P., Jerez, S., Gómez-Navarro, J., García-Valero, J., and Jimenez-Guerrero, P.: Characterization of surface winds over the Iberian Peninsula, *Int. J. Climatol.*, 35, 1007–1026, doi:10.1002/joc.4189, 2014. 3327
- Nogaj, M., Parey, S., and Dacunha-Castelle, D.: Non-stationary extreme models and a climatic application, *Nonlin. Processes Geophys.*, 14, 305–316, doi:10.5194/npg-14-305-2007, 2007. 3337
- Pfahl, S.: Characterising the relationship between weather extremes in Europe and synoptic circulation features, *Nat. Hazards Earth Syst. Sci.*, 14, 1461–1475, doi:10.5194/nhess-14-1461-2014, 2014. 3326, 3335
- Philipp, A., Della-Marta, P., Jacobett, J., Fereday, D., Jones, P., Moberg, A., and Wanner, H.: Long-term variability of day North Atlantic-European pressure patterns since 1850 classified by simulated annealing clustering, *J. Climate*, 20, 4065–4095, 2006. 3326, 3338
- Rodríguez-Puebla, C., Encinas, A. H., García-Casado, L. A., and Nieto, S.: Trends in warm days and cold nights over the Iberian Peninsula: relationships to large-scale variables, *Climatic Change*, 100, 667–684, 2010. 3327
- Sen, P. K.: Estimates of the regression coefficient based on Kendall's tau, *J. Am. Stat. Assoc.*, 63, 1379–1389, 1968. 3331
- Seneviratne, S. I., Corti, T., Davin, E. L., Hirschi, M., Jaeger, E. B., Lehner, I., Orlowsky, B., and Teuling, A. J.: Investigating soil moisture–climate interactions in a changing climate: a review, *Earth-Sci. Rev.*, 99, 125–161, 2010. 3341
- Seubert, S., Fernández-Montes, S., Philipp, A., Hertig, E., Jacobeit, J., Vogt, G., Paxian, A., and Paeth, H.: Mediterranean climate extremes in synoptic downscaling assessments, *Theor. Appl. Climatol.*, 117, 257–275, 2014. 3337

---

**Extreme hot days and atmospheric dynamics**J. A. García-Valero et al.

---

[Title Page](#)[Abstract](#)[Introduction](#)[Conclusions](#)[References](#)[Tables](#)[Figures](#)[◀](#)[▶](#)[◀](#)[▶](#)[Back](#)[Close](#)[Full Screen / Esc](#)[Printer-friendly Version](#)[Interactive Discussion](#)

---

## Extreme hot days and atmospheric dynamics

J. A. García-Valero et al.

---

Title Page

Abstract

Introduction

Conclusions

References

Tables

Figures

◀

▶

◀

▶

Back

Close

Full Screen / Esc

Printer-friendly Version

Interactive Discussion



- Sheridan, S., Lee, C., Allen, M., and Kalkstein, L.: Future heat vulnerability in California, Part I: projecting future weather types and heat events, *Clim. Change*, 115, 1–19, 2012. 3329
- Sousa, P. M., Trigo, R. M., Aizpurua, P., Nieto, R., Gimeno, L., and Garcia-Herrera, R.: Trends and extremes of drought indices throughout the 20th century in the Mediterranean, *Nat. Hazards Earth Syst. Sci.*, 11, 33–51, doi:10.5194/nhess-11-33-2011, 2011. 3341
- 5 Stocker, T., Dahe, Q., and Plattner, G.: Working Group I Contribution to the IPCC Fifth Assessment Report Climate Change 2013, The Physical Science Basis, Cambridge University Press, Cambridge, UK, 2013. 3324, 3326
- Storch, V. and Zwiers, W.: Empirical orthogonal functions, in: *Statistical Analysis in Climatic Research*, Cambridge University Press, Cambridge, UK, 135–192, 1999. 3329
- 10 Stott, P. A.: Attribution of regional-scale temperature changes to anthropogenic and natural causes, *Geophys. Res. Lett.*, 30, 1944–8007, doi:10.1029/2003GL017324, 2003. 3325
- Swingedouw, D., Terray, L., Cassou, C., Voldoire, A., Salas-Mélie, D., and Servonnat, J.: Natural forcing of climate during the last millennium: fingerprint of solar variability, *Clim. Dynam.*, 36, 1349–1364, 2011. 3325
- 15 Trigo, R., García-Herrera, R., Díaz, J., Trigo, I., and Valente, M.: How exceptional was the early August 2003 heatwave in France?, *Geophys. Res. Lett.*, 32, L10701, doi:10.1029/2005GL022410, 2005. 3325, 3331
- Uppala, S., Kallberg, P., Simmons, A., Andra, U., da Costa Beechtold, V., Fiorino, M., Gibson, J., Haseler, J., Hernandez, A., Kelly, G., Li, X., Onogi, K., Saarinen, S., Sokka, N., Allan, R., Andersson, E., Arpe, K., Balmaseda, M., Beljaars, A., van de Berg, L., Bidlot, J., Bormann, N., Caires, S., Chevallier, F., Dethof, A., Dragosavac, M., Fisher, M., Fuentes, M., Sagemann, Holm, E., Hoskins, B., Isaksen, L., Janssen, P., Jenne, R., McNally, A., Mahfouf, J., Mocrette, J., Rayner, N., Saunders, R., Simon, P., Sterl, A., Trenberth, K., Untch, A., Vasiljevic, D., Viterbo, P., and Woollen, J.: The era-40 re-analysis, *Royal Meteorological Society*, 131, 2961–3012, 2005. 3328
- 20 Van den Besselaar, E., Tank, A. K., and Van der Schrier, G.: Influence of circulation types on temperature extremes in Europe, *Theor. Appl. Climatol.*, 99, 431–439, 2010. 3326
- Vautard, R. and Yiou, P.: Control of recent European surface climate change by atmospheric flow, *Geophys. Res. Lett.*, 36, L22702, doi:10.1029/2009GL040480, 2009. 3337
- 30 Ward, J.: Hierarchical grouping to optimize an objective function, *J. Am. Stat. Assoc.*, 58, 236–244, 1963. 3329

- Yiou, P. and Nogaj, M.: Extreme climatic events and weather regimes over the North Atlantic: when and where?, *Geophys. Res. Lett.*, 31, 1–4, 2004. 3326
- Yiou, P., Goubanova, K., Li, Z. X., and Nogaj, M.: Weather regime dependence of extreme value statistics for summer temperature and precipitation, *Nonlin. Processes Geophys.*, 15, 365–378, doi:10.5194/npg-15-365-2008, 2008. 3326
- 5 ZwiERS, F. W., Zhang, X., and Feng, Y.: Anthropogenic influence on long return period daily temperature extremes at regional scales, *J. Climate*, 24, 881–892, 2011. 3325

---

**Extreme hot days and atmospheric dynamics**J. A. García-Valero et al.

---

[Title Page](#)[Abstract](#)[Introduction](#)[Conclusions](#)[References](#)[Tables](#)[Figures](#)[◀](#)[▶](#)[◀](#)[▶](#)[Back](#)[Close](#)[Full Screen / Esc](#)[Printer-friendly Version](#)[Interactive Discussion](#)







## Extreme hot days and atmospheric dynamics

J. A. García-Valero et al.

**Table 4.** Efficiencies before-after the allocation process (in percentage). Efficiencies are from the CTs belonging to the best classification for each region (last column).

Region	CT1	CT2	CT3	CT4	CT5	CT6	CT7	CT8	Classification
SW	53.3–17.6	51.3–44.4	66.7–18.5	31.9–24.8	3.2–0.5	0.0–0.0	20.5–4.9	0.0–0.0	SLP-T850
NWs	46.7–15.4	63.5–54.9	39.8–11.1	38.3–29.8	3.2–0.5	6.6–1.4	38.6–9.2	0.0–0.0	
NWe	25.2–8.3	74.8–64.7	10.2–2.8	21.3–16.5	48.4–7.0	14.3–3.0	41.0–9.8	0.0–0.0	
N	17.0–5.6	80.0–69.2	1.9–0.5	26.6–20.7	25.8–3.7	55.0–11.6	41.0–9.8	0.0–0.0	
NE	26.5–6.7	77.1–72.2	12.0–4.0	45.0–34.0	25.3–8.7	3.1–0.6	59.7–21.5	8.5–0.4	Z500-T850
Cs	3.7–0.9	77.1–72.2	51.3–17.2	42.2–31.9	41.4–14.2	1.0–0.2	6.5–2.3	4.3–0.2	
NWw	50.0–12.6	25.4–23.8	39.3–13.2	27.5–20.8	1.0–0.4	67.7–12.0	3.2–1.2	0.0–0.0	
E	17.9–5.1	19.8–8.8	27.3–12.3	50.0–37.0	2.2–0.3	39.5–6.0	6.3–4.7	91.0–6.7	SLP-Z500

[Title Page](#)
[Abstract](#)
[Introduction](#)
[Conclusions](#)
[References](#)
[Tables](#)
[Figures](#)
[Back](#)
[Close](#)
[Full Screen / Esc](#)
[Printer-friendly Version](#)
[Interactive Discussion](#)




## Extreme hot days and atmospheric dynamics

J. A. García-Valero et al.

Title Page

Abstract

Introduction

Conclusions

References

Tables

Figures



Back

Close

Full Screen / Esc

Printer-friendly Version

Interactive Discussion



**Table 6.** Thresholds of the different CTs used for distance/correlation in the allocating process.

Classification	CT1	CT2	CT3	CT4	CT5	CT6	CT7	CT8
SLP-T850	0.06/−0.26	0.06/0.57	0.06/0.40	0.06/0.67	0.05/0.18	0.08/0.36	0.06/0.61	0.07/0.39
Z500-T850	0.07/0.18	0.05/0.14	0.05/−0.09	0.05/0.02	0.05/−0.06	0.05/0.27	0.06/0.36	0.07/0.31
SLP-Z500	0.06/0.10	0.07/0.59	0.06/−0.12	0.06/0.72	0.06/0.17	0.08/0.47	0.05/0.47	0.08/0.04

## Extreme hot days and atmospheric dynamics

J. A. García-Valero et al.

Title Page

Abstract

Introduction

Conclusions

References

Tables

Figures



Back

Close

Full Screen / Esc

Printer-friendly Version

Interactive Discussion



**Table 7.** Explained variance by the clusters (in %) for the three CT classifications before and after the allocation process.

	Z500-T850	SLP-T850	SLP-Z500
before	49.97	49.65	49.48
after	50.06	47.02	46.59



## Extreme hot days and atmospheric dynamics

J. A. García-Valero et al.

**Table 9.** Trends in the frequency of CTs (days decade<sup>-1</sup>) before/after the allocation process. One (two) asteriks indicate trends at 90 % (95 %) of the confidence level (Mann–Kendall test).

Classification	CT1	CT2	CT3	CT4	CT5	CT6	CT7	CT8	CT9
SLP-T850	0.50**/0.00	0.35**/0.26*	0.45**/0.00	0.00/0.00	0.00/–0.43	0.00/0.51*	0.00/0.00	0.00/0.00	NA/–1.3
Z500-T850	0.28**/0.28	0.45**/0.45**	0.40**/0.00	0.00/0.00	0.00/0.00	0.00/–0.53	0.00/0.80**	0.00/0.00	NA/–0.80
SLP-Z500	0.40**/0.00	0.36*/0.57*	0.00/0.00	0.00/0.00	0.00/0.00	0.00/0.57*	0.00/0.00	0.00/–0.30	NA/–0.50

[Title Page](#)
[Abstract](#)
[Introduction](#)
[Conclusions](#)
[References](#)
[Tables](#)
[Figures](#)
[Back](#)
[Close](#)
[Full Screen / Esc](#)
[Printer-friendly Version](#)
[Interactive Discussion](#)




---

**Extreme hot days and  
atmospheric  
dynamics**J. A. García-Valero et al.

---

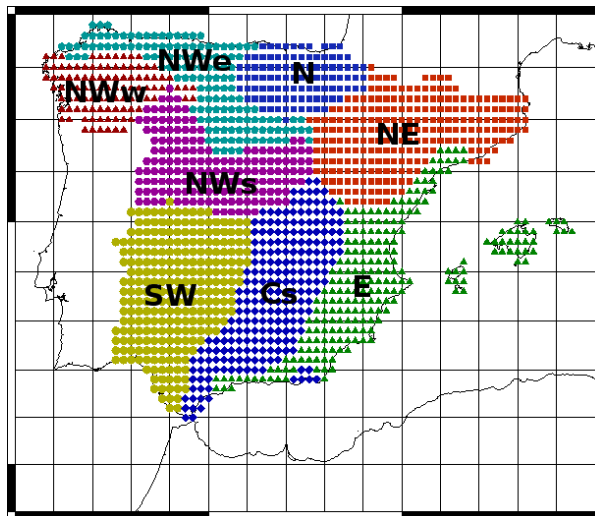


**Figure 1.** Eight regions obtained as result of the regionalization process applied to the summer maximum daily temperatures (16 June to 15 September) of the Spain02 database (Herrera et al., 2010) for the period 1951–2008.

[Title Page](#)[Abstract](#)[Introduction](#)[Conclusions](#)[References](#)[Tables](#)[Figures](#)[◀](#)[▶](#)[◀](#)[▶](#)[Back](#)[Close](#)[Full Screen / Esc](#)[Printer-friendly Version](#)[Interactive Discussion](#)

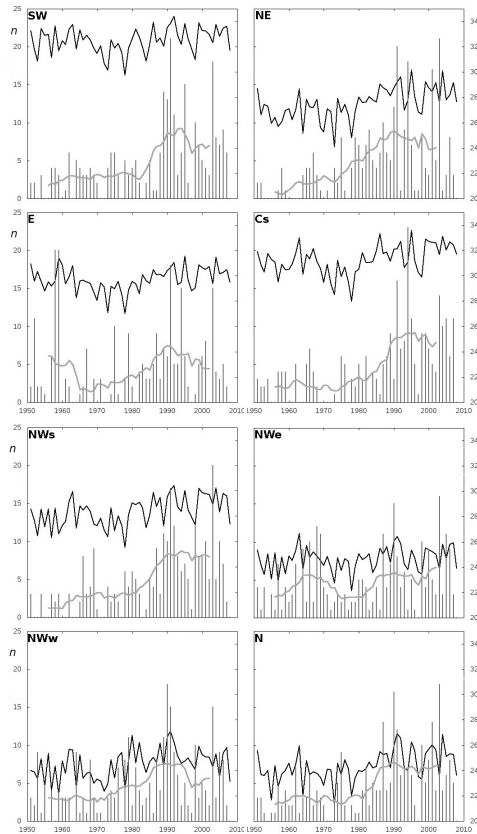


**Figure 2.** Temporal evolution of the eight regional series. Regional annual series of  $T_{\max}$  are indicated by the black curve, whereas annual frequency of EHD is depicted by vertical bars for the different regions. The grey curve shows the running mean of EHDs using a window of 10 years. Left axis represents EHD annual frequency while right axis corresponds to the temperature scale in °C.

**Extreme hot days and atmospheric dynamics**

J. A. García-Valero et al.

Title Page

Abstract	Introduction
Conclusions	References
Tables	Figures

◀
▶

◀
▶

Back	Close
------	-------

Full Screen / Esc

Printer-friendly Version

Interactive Discussion



## Extreme hot days and atmospheric dynamics

J. A. García-Valero et al.

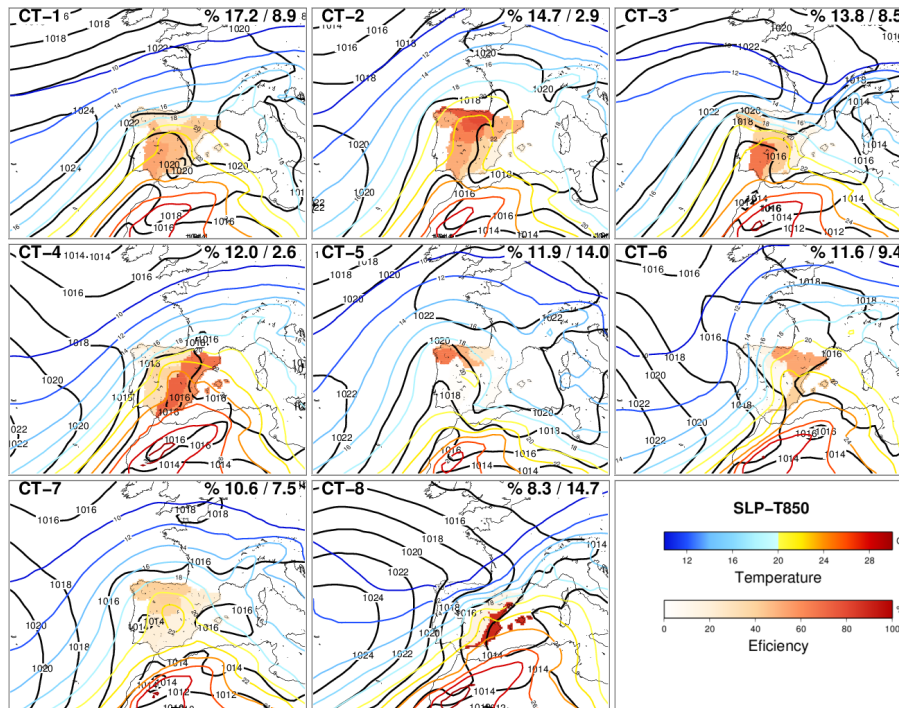


**Figure 3.** Centroids of the CTs for the SLP-T850 classification. SLP and T850 are represented by contours, black lines for SLP and colour lines for T850. Shading denotes the regional EHD efficiencies associated with each CT. The top left corner shows the number of the represented CT. Right corner indicates the frequency (in percentages) of each CT, before/after of applying the allocating method (Subsec 5.1).

Title Page

Abstract

Introduction

Conclusions

References

Tables

Figures

◀

▶

◀

▶

Back

Close

Full Screen / Esc

Printer-friendly Version

Interactive Discussion



## Extreme hot days and atmospheric dynamics

J. A. García-Valero et al.

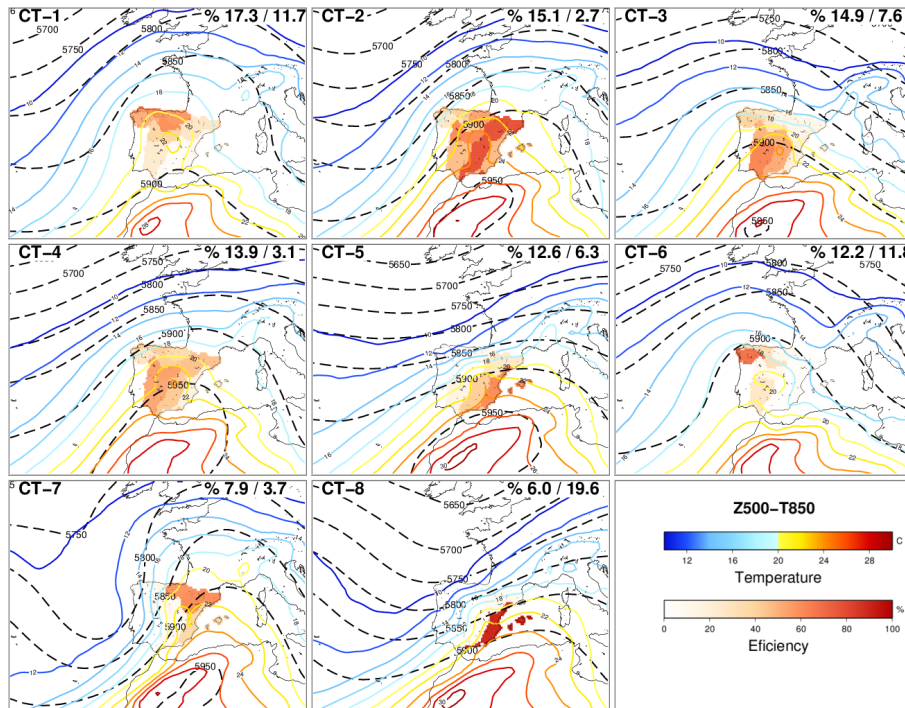


**Figure 4.** Same as Fig. 3 but for the Z500-T850 classification. Z500 and T850 are represented by isohypsals (shaded black lines) and isothermals (colour lines).

Title Page

Abstract

Introduction

Conclusions

References

Tables

Figures



Back

Close

Full Screen / Esc

Printer-friendly Version

Interactive Discussion



## Extreme hot days and atmospheric dynamics

J. A. García-Valero et al.

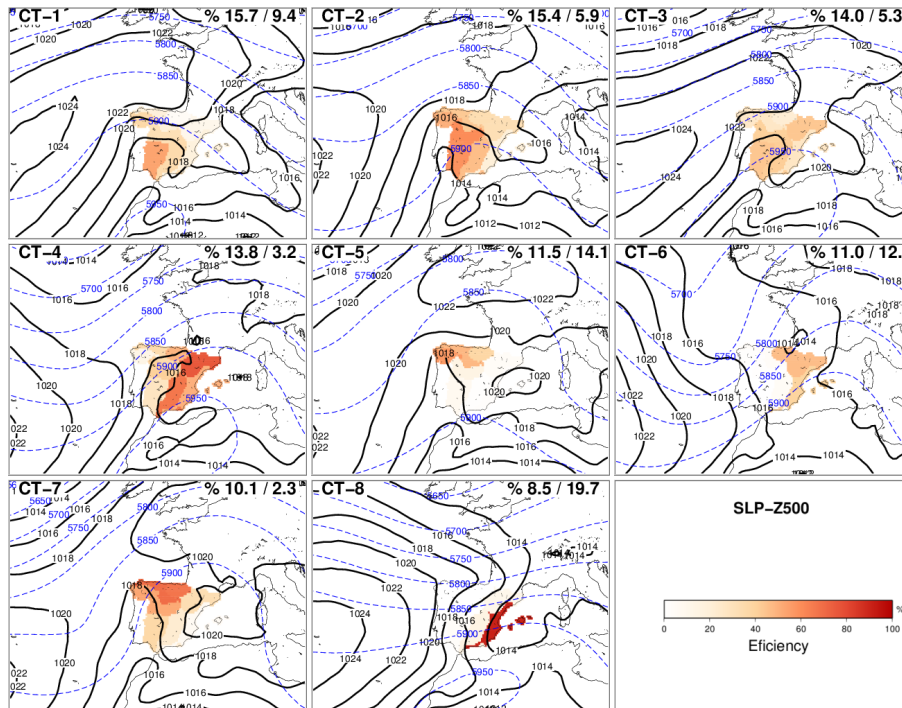


**Figure 5.** Same as Fig. 3 but for the SLP-Z500 classification. ZLP and Z500 are represented by isobars (black lines) and isohypsas (blue shaded lines).

Title Page

Abstract

Introduction

Conclusions

References

Tables

Figures



Back

Close

Full Screen / Esc

Printer-friendly Version

Interactive Discussion



## Extreme hot days and atmospheric dynamics

J. A. García-Valero et al.

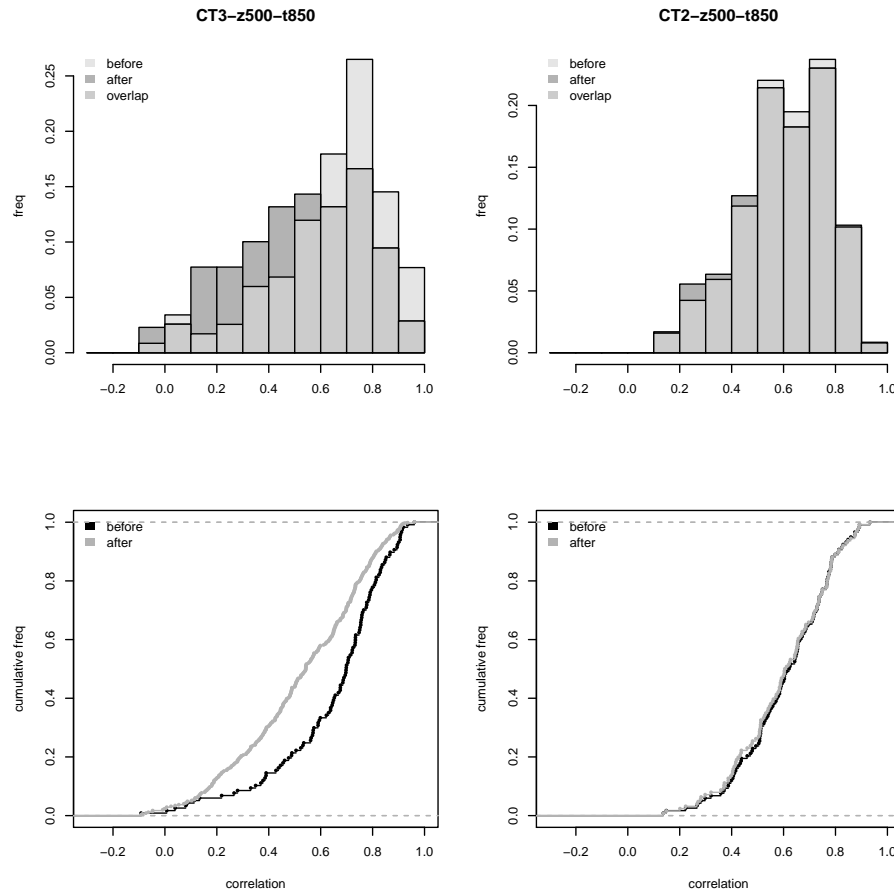


**Figure 6.** Histograms and Empirical Cumulative Distribution Functions of the correlations for CT3-Z500-T850 (left) and CT2-Z500-T850 (right). Each panel shows the populations before and after the allocation process.

[Title Page](#)  
[Abstract](#)   [Introduction](#)  
[Conclusions](#)   [References](#)  
[Tables](#)   [Figures](#)  
◀   ▶  
◀   ▶  
[Back](#)   [Close](#)  
[Full Screen / Esc](#)  
[Printer-friendly Version](#)  
[Interactive Discussion](#)



## Extreme hot days and atmospheric dynamics

J. A. García-Valero et al.

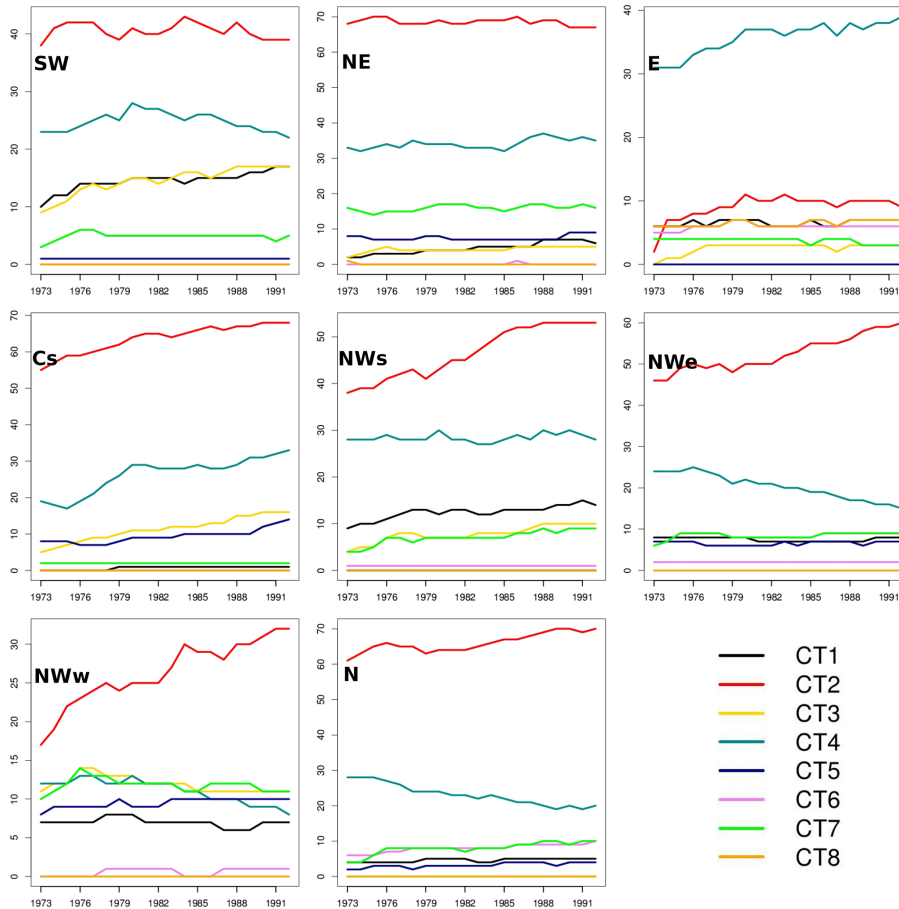


**Figure 7.** Within Type variations. Moving average efficiencies calculated by 31-year periods by Efficiency WT variations. Moving average efficiencies (31-years) of the CTs composing the best CT classification for each region after the allocation process.

Title Page

Abstract Introduction

Conclusions References

Tables Figures

⏪ ⏩

◀ ▶

Back Close

Full Screen / Esc

Printer-friendly Version

Interactive Discussion

